

## Structural evolution of the Lanterman Metamorphic Complex, northern Victoria Land, Antarctica

MICHAEL SANDIFORD

Department of Geology  
University of Melbourne  
Parkville 3052  
Victoria, Australia

**Abstract** The metamorphic rocks of the Lanterman and Salamander Ranges in northern Victoria Land, termed the Lanterman Metamorphic Complex, are composed predominantly of semi-pelitic metasediments and subordinate pelitic, calcareous and conglomeratic metasediments, and mafic schists of presumed volcanic origin. Intrusive rocks include metamorphosed basic dikes, metatonalites, and Granite Harbour Intrusives. Talc schists occur as small pods in highly deformed zones in the eastern Lanterman Range and separate zones of distinct structural and metamorphic character. In the western terrane, amphibolite facies metamorphism accompanied the development of a steeply dipping schistosity ( $S_1$ ) and a vertical mineral elongation lineation. Bedding ( $S_0$ ) was transposed within  $S_1$ . Subsequent deformation during retrograde metamorphism resulted in mesoscopic crenulate structures ( $F_2$  and  $F_3$ ) in  $S_1$ . The development of  $S_1$  and its crenulation is regarded as part of a continuous deformation cycle broadly coeval with the emplacement of the Granite Harbour Intrusives during the early Paleozoic Ross Orogeny. In the eastern terrane, in which no intrusives occur, greenschist facies metamorphism accompanied the development of large-scale upright folds in metaconglomerates.  $S_0$  is not transposed in the axial schistosity which is subvertical, trends NNW, and contains a near-vertical lineation defined by pebble elongation. Juxtaposition of the two contrasting terranes probably accompanied the emplacement of the talc schists during the Ross Orogeny.

**Keywords** Antarctica; northern Victoria Land; Lanterman Metamorphic Complex; Granite Harbour Intrusives; Husky Conglomerate; structures; tectonics

### INTRODUCTION

The Lanterman and Salamander Ranges in northern Victoria Land consist predominantly of amphibolite grade metamorphics (Dow & Neall 1974; Kleinschmidt 1981; Tessensohn et al. 1981; Bradshaw et al. 1982; Grew & Sandiford 1982). These metamorphics, together with most other high-grade metamorphics in northern Victoria Land, have previously been included in the Wilson Group. However, recently it has been recognised that the Lanterman and Salamander Metamorphics form a distinct stratigraphic and structural entity (Tessensohn et al. 1981; Grew & Sandiford 1982; Bradshaw & Laird 1983), and by an agreement reached at the Fourth International Symposium of Antarctic Earth Sciences in Adelaide, Australia, in August of 1982, they are referred to as the Lanterman Metamorphic Complex. Previous reconnaissance studies have shown that the Lanterman Metamorphic Complex forms one of the most complex structural entities within northern Victoria Land (Dow & Neall 1974; Kleinschmidt 1981; Kleinschmidt & Skinner 1981; Tessensohn et al. 1981; Bradshaw et al. 1982) and is critical to any interpretation of the tectonic evolution of northern Victoria Land.

Two opposing hypotheses have been proposed for the origin of the Lanterman Metamorphic Complex (Tessensohn et al. 1981; Bradshaw et al. 1982). Bradshaw et al. (1982) considered the complex to be a Precambrian terrain which forms the basement to the Cambro-Ordovician Bowers Supergroup. Tessensohn et al. (1981) considered the Lanterman Metamorphics to be a metamorphosed segment of the early Paleozoic Ross orogen and a higher grade equivalent of other units in the Ross orogen, such as the Bowers Supergroup. The principal observations in support of these hypotheses relate to the nature of the contact between deformed metaconglomerates in the Lanterman Range, described by Wodzicki et al. (1982), and the Husky Conglomerate (Laird et al. 1982). Laird et al. (1982) inferred that the Husky Conglomerate unconformably overlies the Lanterman Metamorphics (Wilson Group), which, at the type locality in a saddle between Reilly Ridge and a spur leading eastwards from Mount Bernstein, includes both felsic and mafic metaconglomerates. Until recently, the stratigraphic affinity of the Husky Conglomerate was uncertain. Laird & Bradshaw

Received 9 January 1984, accepted 14 December 1984

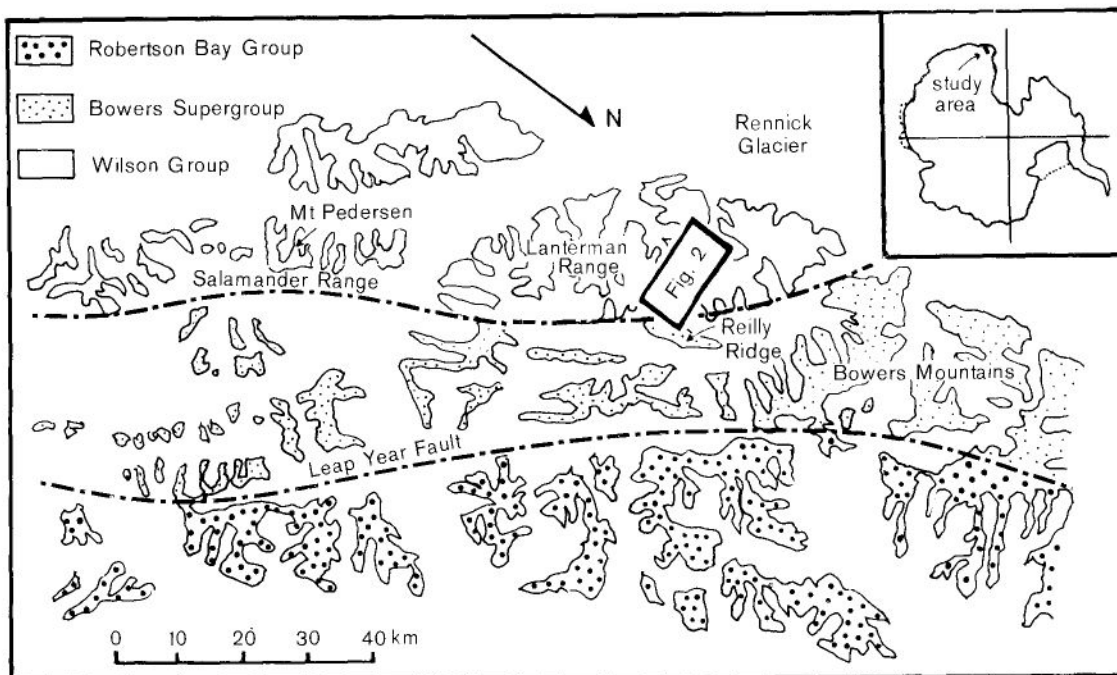


Fig. 1 Geological map showing the distribution of basement units in northern Victoria Land.

(1983) regarded it as similar to, and as a possible equivalent of, conglomerates in the Cambrian-aged Sledgers Group which forms the base of the Bowers Supergroup. Bradshaw et al. (1982) suggested that the deposition of the Husky Conglomerate postdated the principal structures in the Lanterman Metamorphics, and that deformation and metamorphism of the Lanterman Metamorphics occurred in the Precambrian. In contrast, Tessensohn et al. (1981, p. 53) concluded that the Husky Conglomerate forms part of a conformable metasedimentary sequence within the Lanterman Metamorphics (Wilson Group). Furthermore, these authors noted that the structures in the Lanterman Metamorphics are parallel to, and thus probable equivalents of, structures in the Bowers and Robertson Bay Groups, and that the Lanterman Metamorphics were similar in composition to lower grade sediments in the Bowers Supergroup. Additional evidence for Paleozoic tectonism in the Lanterman Metamorphic Complex was provided by Wyborn (1981) and Tessensohn et al. (1981), who suggested that granite stocks and veins in the Lanterman Metamorphics were syntectonic with the major tectonism. These granites have yielded early Paleozoic (480–490 Ma) Ross Orogeny ages equivalent with Granite Harbour Intrusives elsewhere in northern Victoria Land (Kreuzer et al. 1981).

In light of the above arguments, the relationships between the various conglomerates and other metamorphic rocks in the Lanterman Range, and the timing of intrusion of the Granite Harbour Intrusives into these metamorphics, are critical to models of the tectonic evolution of northern Victoria Land, and are the principal questions addressed in this study.

This paper reports the results of structural studies based on detailed traverses across the central Lanterman Range in the vicinity of Mount Bernstein and in the Salamander Range near Mount Pedersen (Fig. 1). Informal names for geographical features that have not yet been accepted by the U.S. Board of Geographic Names have been placed in quotation marks.

#### STRATIGRAPHY AND PETROGRAPHY

Several metasedimentary and metavolcanic rock types and a variety of intrusives, both metamorphosed and unmetamorphosed, are exposed in the Lanterman Metamorphic Complex. Six stratigraphic units (units 1–6, Fig. 2) have been mapped in the Mount Bernstein region. The gradational contacts between most of these units imply that their distinction is somewhat arbitrary. However, the recognition of these units provides a useful basis

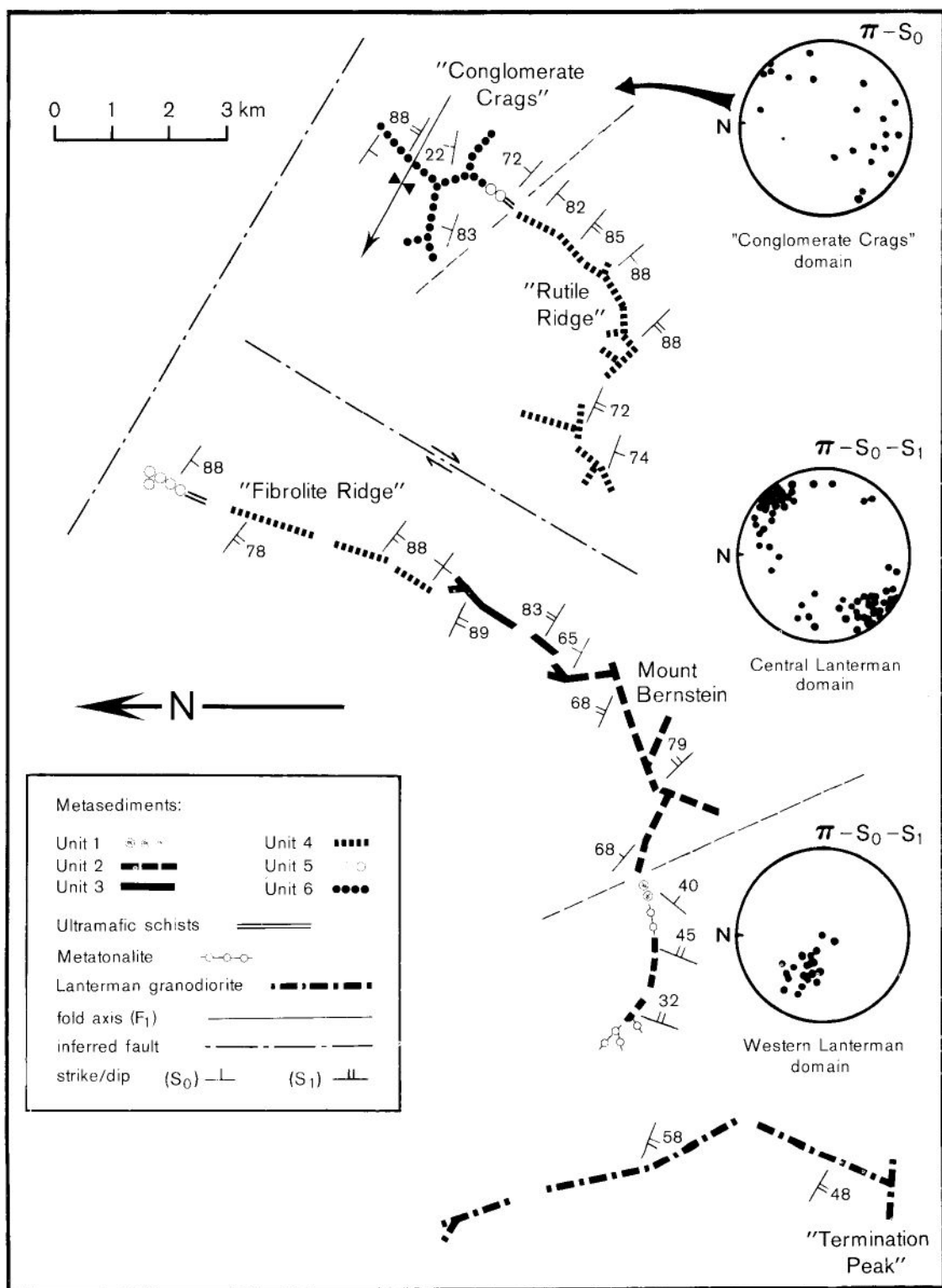


Fig. 2 Geological map of the Mount Bernstein region, Lanterman Range, northern Victoria Land.

Sig 5

for establishing the major structure in the Lanterman Ranges. No evidence for an unconformity between any of these units was found, and the structural relationships suggest that many of the rock types form part of a conformable supracrustal sequence. However, tectonic transposition has obscured many of the primary contacts and precludes the unambiguous interpretation of many of the primary stratigraphic relationships. Moreover, the contact represented by an important sedimentological break between metaconglomerates (units 5 and 6) and semipelitic schists (unit 4) in the eastern part of the Lanterman Range is obscured by a series of highly deformed talc-serpentine schists. The contrasting styles of sedimentation on either side of these talc schists suggest the possibility of two distinct stratigraphic series in the Lanterman Metamorphic Complex.

Stratigraphic repetition has been observed only in the easternmost unit (unit 6) in the Lanterman Range, suggesting that the greater proportion of the sequence is essentially monocinal. Younging evidence has been observed only in unit 6, and thus stratigraphic superposition is unknown throughout the greater part of the Lanterman Range.

The Lanterman Metamorphics preserve assemblages indicative of metamorphism in upper greenschist to middle amphibolite facies conditions (Grew & Sandiford 1982). Grade increases westwards across the Lanterman Ranges, with a significant break between epidote - albite - hornblende/actinolite assemblages in the metaconglomerates (units 5 and 6) in the "Conglomerate Crags" region and andesine/labradorite - hornblende assemblages to the west of the talc schists (Fig. 2). In the Mount Bernstein region, migmatites and fibrolite-K-feldspar assemblages occur in pelitic schists. Grew & Sandiford (1984) estimated the maximum conditions attained near Mount Bernstein to be 650–700°C at 5.5–6.4 kbar. An earlier, higher pressure metamorphic phase is indicated in the Mount Bernstein region by the occurrence of relic kyanite and staurolite along "Fibrolite Ridge" (Grew & Sandiford 1984, 1985). All outcrops visited in the Salamander Ranges appear to be sillimanite grade.

#### Supracrustal rocks

The characteristic features of the metasedimentary and metavolcanic rock types observed in the Lanterman Metamorphic Complex (Fig. 2), including each of the six stratigraphic units observed in the Mount Bernstein region, are described below.

**Unit 1** is composed of fine-grained (0.5–2 mm) granoblastic calcsilicate gneisses, which occur as thick (>20 m), compositionally homogeneous units within biotite schists to the west of Mount Bern-

stein (Fig. 2). The calcsilicate gneisses are composed predominantly of diopside, quartz, plagioclase, and sphene. Calcic amphibole is a common accessory phase.

**Unit 2** metasediments are monotonous semipelitic schists containing subordinate calcsilicate lenses. They crop out with an exposed thickness in excess of 1.5 km between the eastern flank of Mount Bernstein and the calcsilicates of unit 1 (Fig. 2). The unit 2 schists are composed principally of biotite, quartz, intermediate plagioclase, diopside, microcline, and/or calcite with accessory zircon and apatite. Migmatites (Fig. 3C) are locally developed in more aluminous compositions which include muscovite and sillimanite in addition to biotite, plagioclase, microcline, and quartz. Contacts between microcline and fibrolitic sillimanite are only locally preserved. More typically, fibrolite is enclosed within muscovite. Numerous 1–5 cm thick calcsilicate lenses are within the biotite schists (Fig. 3A, B). Primary metamorphic components in the calcsilicates include quartz, plagioclase, diopside, calcite, hornblende, and sphene. Prehnite, Ca-amphibole, chlorite, and epidote are common secondary alteration products.

**Unit 3** metasediments are medium-grained (2–5 mm) pelitic schists forming the dominant rock type exposed along the western end of "Fibrolite Ridge" (Fig. 2). They are typically composed of biotite, quartz, microcline, muscovite, sillimanite, and intermediate plagioclase. Garnet and magnetite are locally present. Sillimanite is common, typically as needles enclosed within muscovite, but at places in contact with K-feldspar. Kyanite occurs as a relic of an earlier metamorphic stage totally enclosed in plagioclase in a fibrolite-bearing schist east of Mount Bernstein (Grew & Sandiford 1984). Biotite is frequently altered to chlorite, and plagioclase is altered to sericite.

**Unit 4** comprises a monotonous sequence of medium-grained (2–8 mm) semipelitic schists and subordinate amphibolite pods and lenses of presumed volcanic origin. Unit 4 crops out with an exposed thickness of 750 m along the western end of "Rutile Ridge" and along the eastern end of "Fibrolite Ridge" (Fig. 2). The metasediments are composed principally of quartz, biotite, muscovite, intermediate plagioclase, and/or calcite. Sphene, apatite, and epidote are common accessory phases. Chlorite occurs as secondary alteration of biotite, especially in areas of  $S_3$  crenulation. The "Rutile Ridge" schists contain numerous lenticular quartz segregation enclosed within the schistose foliation. Plagioclase, rutile, and diopside occur as accessory phases in these quartz veins. Hornblende amphibolites, and associated rock types, occur as 2–4 m wide pods and lenses in a 200 m thick zone near

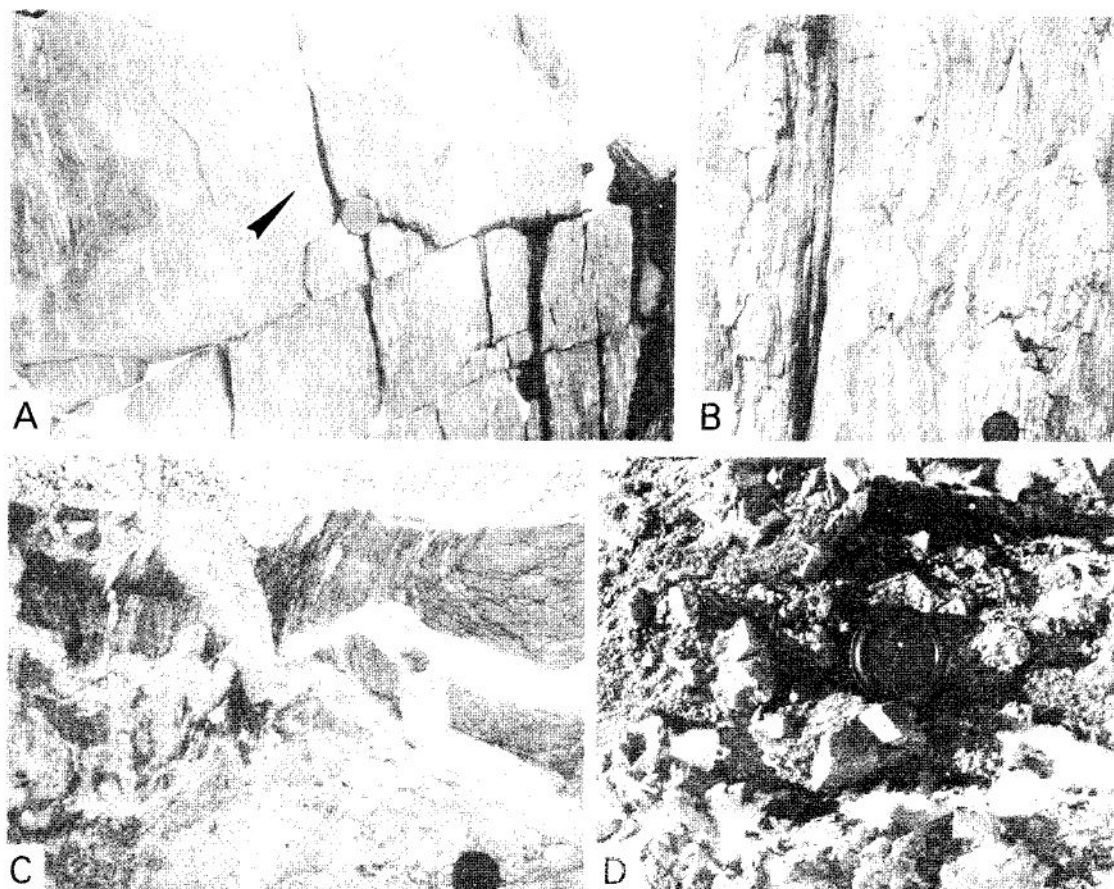


**Fig. 3** Metamorphic rocks in the Lanterman Range. **A** Relict F hinges (arrowed) in light coloured calc-silicate lenses occurring as transposed layers within biotite schist, unit 2, Mount Bernstein. **B** Subhorizontal boudinage of calc-silicate lenses in a matrix of biotite schist, Mount Bernstein. **C** Migmatites in biotite-biotite schists, unit 2, Mount Bernstein. **D** Talc - serpentinite - magnesite rock with magnesite rhombs weathered out, unit 6, "Rabbit Ridge".

the eastern end of unit 4. The principal components of these pods are hornblende, plagioclase, epidote, quartz, diopside, microcline, and/or sphene.

**Unit 5** forms a distinctive 60 m thick association, composed predominantly of felsic metaconglomerates with subordinate intercalated metapsammites (Fig. 4), cropping out on the western flank of "Conglomerate Crags" and at the eastern tip of "Tibolite Ridge" (Fig. 2). The dominant clast type of this essentially monometic conglomerate consists of quartz and albite, with accessory chlorite, muscovite, and/or calcite. The felsic clasts are characteristically flattened into oblate spheroids (Fig. 4B, C). Rare clasts of biotite and actinolite-chlorite schist occur towards the eastern end of the unit. The matrix in the metaconglomerate is composed

of biotite, quartz, plagioclase, Ca-amphibole, muscovite, chlorite, and/or epidote, and it is similar in mineralogy to interlayered metapsammites. The metapsammites are typically  $\sim 1$  m thick, although one layer, which demarcates the western margin of unit 5, is 15 m thick.

**Unit 6** is composed predominantly of a polymict metaconglomerate, in which the dominant clast type (80-90% of clasts) is amphibolite (Fig. 5). It crops out in scattered exposures in the Lanterman Metamorphics in the Reilly Ridge - "Conglomerate Crags" region. The across-strike outcrop extent of this unit is nearly 2 km, but its true thickness is substantially less (approx. 700 m) due to repetition about a large syncline exposed in the cliffs at "Conglomerate Crags" (Fig. 5C). The dominant clast type and matrix assemblages are similar,

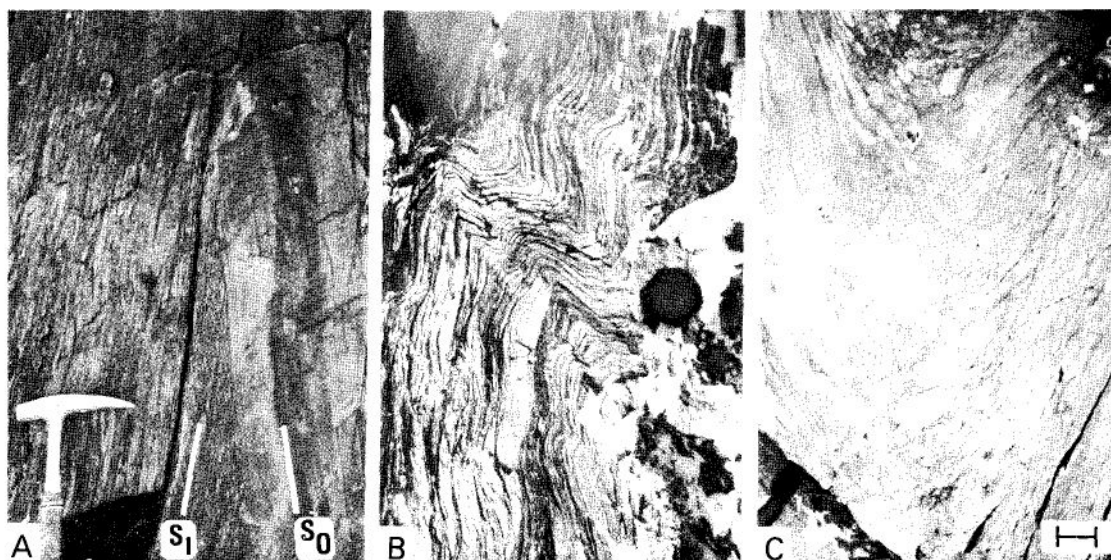


**Fig. 4** Felsic metaconglomerates (unit 5), "Conglomerate Crags". A Discordance between  $S_0$  (defined by sedimentary laminations in psammites) and  $S_1$  (defined by flattened metaconglomerate clasts). As the photograph is viewed from the south, synclinal vergence is to the east. C  $F_3$ , folds showing fragmentation of the metaconglomerate fabric in the hinge. Bar scale is 5 cm.

varying only in the proportion of hornblende, quartz, biotite, albite, epidote, and chlorite. Clasts of granodiorite, marble, and vein quartz were also found. Numerous thin amphibole, chlorite, and biotite-rich metapsammites occur within this metaconglomerate (Fig. 5D, E). Cross bedding is preserved in some of these psammitic intercalations.

#### Salamander Ranges

The dominant rock type in the Salamander Range is a fine-medium-grained biotite schist. It is composed of biotite, quartz, plagioclase, microcline, and/or muscovite. Fibrolitic and garnet-bearing biotite schists are locally common and suggest comparison with unit 3 in the Lanterman Range. However, the occurrence of a distinctive garnet-bearing calcsilicate gneiss in the vicinity of Mount Pedersen (composed of quartz, diopside, plagioclase, grossular, and epidote) suggests that the Salamander outcrops represent a distinct section through the Lanterman Metamorphics.

#### Intrusive rocks

A number of distinct pre-, syn-, and post-tectonic intrusive events have been identified. These include rocks ranging from ultrabasic through to acidic in composition.

Metamorphosed mafic hornblende-bearing dikes are relatively common in the Salamander Ranges. Intrusive contacts are locally preserved between these hornblende rocks and the country rocks (Fig. 6A). More typically, primary contacts with the metasediments are transposed. The dikes typically exhibit medium-coarse grained (3–10 mm) granoblastic textures. Their mineralogical composition is variable; hornblende forms the principal component and plagioclase and biotite are common. These dikes are most probably related to more massive plagioclase-hornblende-quartz-biotite gneisses (metatonalite) which crop out as subconcordant layers, > 30 m thick, in the western part of the Lanterman Range (Fig. 2) and in the Salamander Range. Although intrusive contacts with the adjacent metasediments were not found, the coarse grain-size (typically 5–10 mm, but occasionally up to 100 mm) suggests an intrusive origin. The Lanterman metatonalite shows a foliated granoblastic fabric (Fig. 6B), suggesting more thorough recrystallisation than is apparent in nearby granites and granodiorites. Pronounced compositional zoning is apparent in the Salamander metatonalite which crops out on a ridge some 5 km north of Mount Pedersen. The zoning is manifest as an eastward gradation from hornblendite to a hornblende-plagioclase-quartz rock in which individual hornblende crystals exceed 10 cm in length (Fig. 6C).

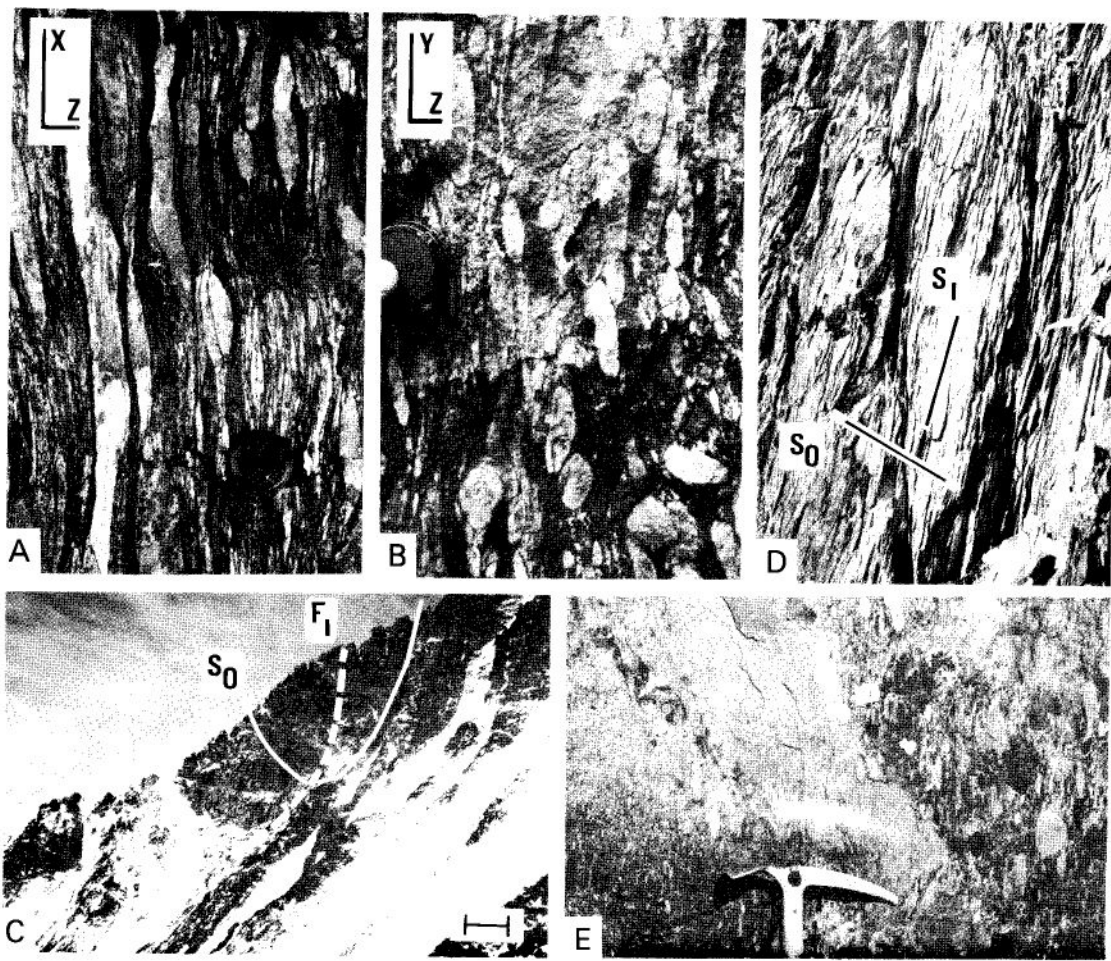


**Fig. 5** Mafic metaconglomerates (unit 6), "Conglomerate Crags". **A** XZ profile of metaconglomerate with an unusually high proportion of felsic clasts. **B** YZ profile of the metaconglomerate depicted in Fig. 4A. **C**  $F_1$  fold (solid line) in north-facing cliffs at "Conglomerate Crags"; the curvature of axial trace (dashed line) is due to upward steepening of the cliff face. Bar scale represents approximately 5 m on horizon. **D**  $S_1/S_0$  intersection in easternmost outcrops at "Conglomerate Crags". The outcrop is viewed from the north, and thus synclinal vergence is to the west. Bar scale is 40 cm. **E** Intercalated chlorite-amphibole schists (metapsammites) and conglomerate near the hinge of the  $F_1$  syncline.

A single-olivine bearing ultramafic rock has been recorded from the Salamander Range. The rock also contains abundant secondary chlorite, talc, and serpentine, and as such may represent a less-altered variety of serpentine-, chlorite-, and talc-bearing rocks which occur as thin highly tectonised layers and pods (<4 m thick) within the unit 4 metasediments on "Fibrolite Ridge" and "Rutile Ridge" (Fig. 2). The thickest unit, which includes a spectacular talc-serpentine-magnesite rock (Fig. 3D), crops out over a 40 m thick interval between the metaconglomerates (unit 5) and semipelitic schists of unit 4, between "Conglomerate Crags" and

"Rutile Ridge". Distinctive ultramafic mineralogical associations in this outcrop include: talc - anthophyllite - Ca amphibole - phlogopite - chlorite; chlorite - talc - actinolite - biotite; and serpentine - talc - tremolite - magnesite. A similar unit, with somewhat more restricted parageneses, occurs near the eastern end of "Fibrolite Ridge" where it also separates metaconglomerates from semipelitic schists (Fig. 2). The talc schists are intensely deformed and their contacts with the metasediments are now tectonic.

Granitoid rocks, including tonalite, granodiorite, and granite, occur in thin discordant veins

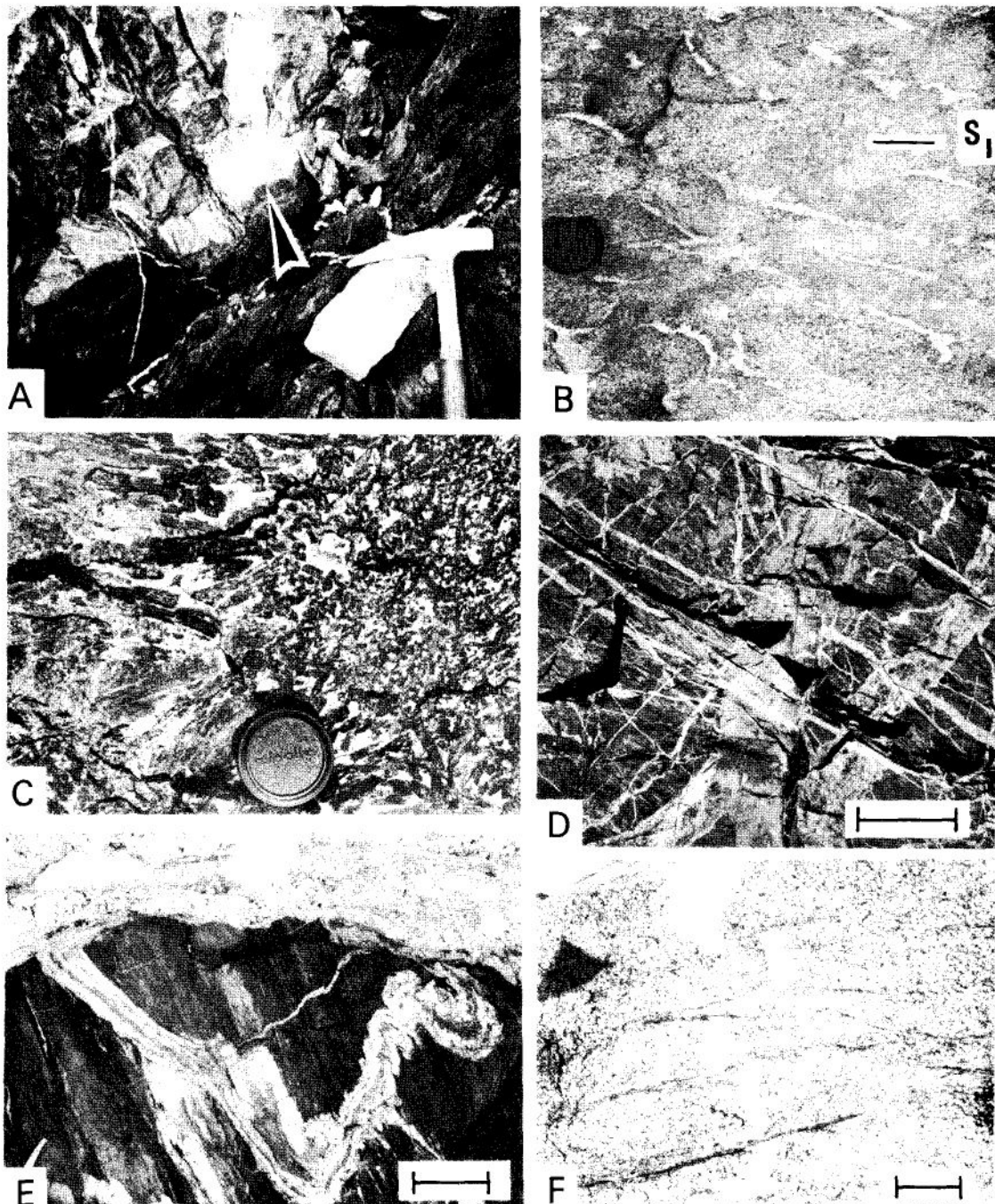


**Fig. 6** Intrusive rocks. **A** Intrusive contact (arrowed) between metamorphosed ultrabasic dike (hornblendite) and diopside-bearing calcsilicates, ridge immediately north of Mount Pedersen. **B**  $S_1$  gneissic foliation formed at an oblique angle to plagioclase-quartz veins in metatonalite, western Lanterman Range. **C** Exaggerated grain growth in hornblende metatonalite, Salamander Ranges. **D** Multiple crosscutting granite and granodiorite dikes, ridge immediately north of Mount Pedersen. Bar scale is 2 m. **E** Two pegmatites both containing weak  $S_1$  fabrics but showing variable development of  $F_1$  folds, Mount Bernstein. Bar scale is 250 cm. **F** Tectonic foliation displaces late-stage aplite veins in Lanterman Granodiorite, "Termination Peak". Bar scale is 5 cm.

throughout the Lanterman and Salamander Ranges (Fig. 6D, E). The only sequences devoid of granite veins are units 5 and 6 at "Conglomerate Crags". A large, composite intrusive body in the western Lanterman Range is termed the Lanterman Granodiorite. The abundance of dikes increases systematically westwards towards the Lanterman Granodiorite which is, therefore, regarded as coeval with the dikes. The Lanterman Granodiorite consists predominantly of hornblende biotite-bearing granodiorite and tonalite with numerous biotite-rich xenoliths. A complex intrusive history is indicated by subordinate granitic layers within the dominant granodiorite. Syntectonic emplacement of the Lanterman Granodiorite and associated dikes is indicated by: (1) a foliation defined by dimensional elongation of xenoliths; (2) incipient polygonisation of quartz; and (3) locally developed tectonic foliations (Fig. 6F).

Granitoid intrusives in Wilson Group metamorphics throughout northern Victoria Land have been collectively referred to as the Granite Harbour Intrusives (Sturm & Carryer 1970). The Granite Harbour Intrusives are typically peraluminous granites and generally contain tourmaline and/or muscovite (Wyborn 1981). The occurrence of hornblende in the Lanterman Granodiorite distinguishes it from other Granite Harbour Intrusives (Wyborn 1981), and the affinities of the Lanterman Granodiorite remain obscure. However, Rb-Sr isotope data indicate an emplacement age of 470–490 Ma (Kreuzer et al. 1981) which is similar to ages of other Granite Harbour Intrusives (Wyborn 1981).

## GENERAL STRUCTURAL RELATIONSHIPS

The structure of the Lanterman Metamorphics is dominated by a pervasive northwest-trending, steep-dipping foliation ( $S_1$ ). This foliation formed during the crystallisation of the highest grade assemblages and is developed in all stratigraphic units observed in the Lanterman Ranges, including the metaconglomerates in the "Conglomerate Crags" region (Fig. 2). This foliation, and the associated lineation ( $L_1$ ), is axial to first generation folds ( $F_1$ ) and is folded and crenulated about second ( $F_2$ ) and third ( $F_3$ ) generation folds, which vary from mesoscopic kinks and crenulations to macroscopic flexures, with amplitudes in excess of 100 m.

Structural relationships in the Lanterman Metamorphic Complex can be divided into three groups:  $S_1$ ,  $L_1$  and  $F_1$ ;  $S_2$ ,  $L_2$  and  $F_2$ ; and  $S_3$ ,  $L_3$  and  $F_3$  (where the subscript correlates synchronous structural elements); correspondingly, the associated deformation events are designated  $D_1$ ,  $D_2$  and  $D_3$ .

Four structural domains have been distinguished on the basis of regional variations in the style and

geometry of the  $S_1$  schistosity, its relationship to the compositional layering, the distribution of macroscopic folds, and the metamorphic grade. A major structural discontinuity exists between the central Lanterman, western Lanterman, and Salamander domains (in which primary compositional layering ( $S_0$ ) is transposed in the  $S_1$  schistosity), and the "Conglomerate Crags" domain (in which  $S_0$  is not transposed). A regional significance is attached to this discontinuity, which coincides with the talc schists between unit 4 and unit 5, because it is accompanied by marked changes in metamorphic grade, intrusive history, and sedimentology. The geometry distinctive of each of the four domains is illustrated in Fig. 7. The structural characteristics of each domain are described below.

### The central Lanterman domain

In the Mount Bernstein region, the primary compositional layering of the metasediments is transposed on a mesoscopic scale within the plane of a pervasive northwest-trending, steep-dipping schistosity and gneissosity ( $S_1$ ). Macroscopic repetitions of the stratigraphy have not been observed, and it is presumed that this domain forms the limb region of a large-scale  $F_1$  structure. However, the lack of recognised facing and vergence in this domain implies that macroscopic folds may have been overlooked.

In biotite schists,  $S_1$  is defined by the preferred orientation of muscovite and biotite (but not chlorite), and in calcsilicates it is defined by a gneissic layering resulting from the transposition of compositional layers (Fig. 3A).  $S_1$  invariably contains a steeply plunging lineation ( $L_1$ ) defined by the preferred dimensional elongation of minerals and mineral aggregates.  $L_1$  is perpendicular to the subhorizontal boudin necks in calcsilicates (Fig. 3B), and in quartz veins, and is therefore regarded as an extension lineation. Mesoscopic  $F_1$  folds, to which  $S_1$  is axial, occur as: (1) steeply plunging interfolia, isoclinal closures within relic compositional layers; (2) tight to isoclinal folds in quartz veins, in which the fold axes are generally parallel to  $L_1$  (Fig. 8A), and (3) open variably oriented folds in quartz dikes (Fig. 6B and 8B). In outcrops where  $S_1$  is absent in all three fabric elements, the corresponding  $F_1$  folds are more tightly folded than the  $F_2$  and  $F_3$  folds, which in turn are more tightly folded

(Fig. 6C, D). An early-folded planar fabric element is locally preserved in the hinge regions of  $F_1$  folds in quartz veins. It is folded along with the quartz veins and is partially recrystallised in the plane of the  $S_1$  axial fabric. Thus, the early fabric represents deformation predating the formation of  $F_1$  folds in the quartz veins. However, the early fabric preserves identical assemblages to

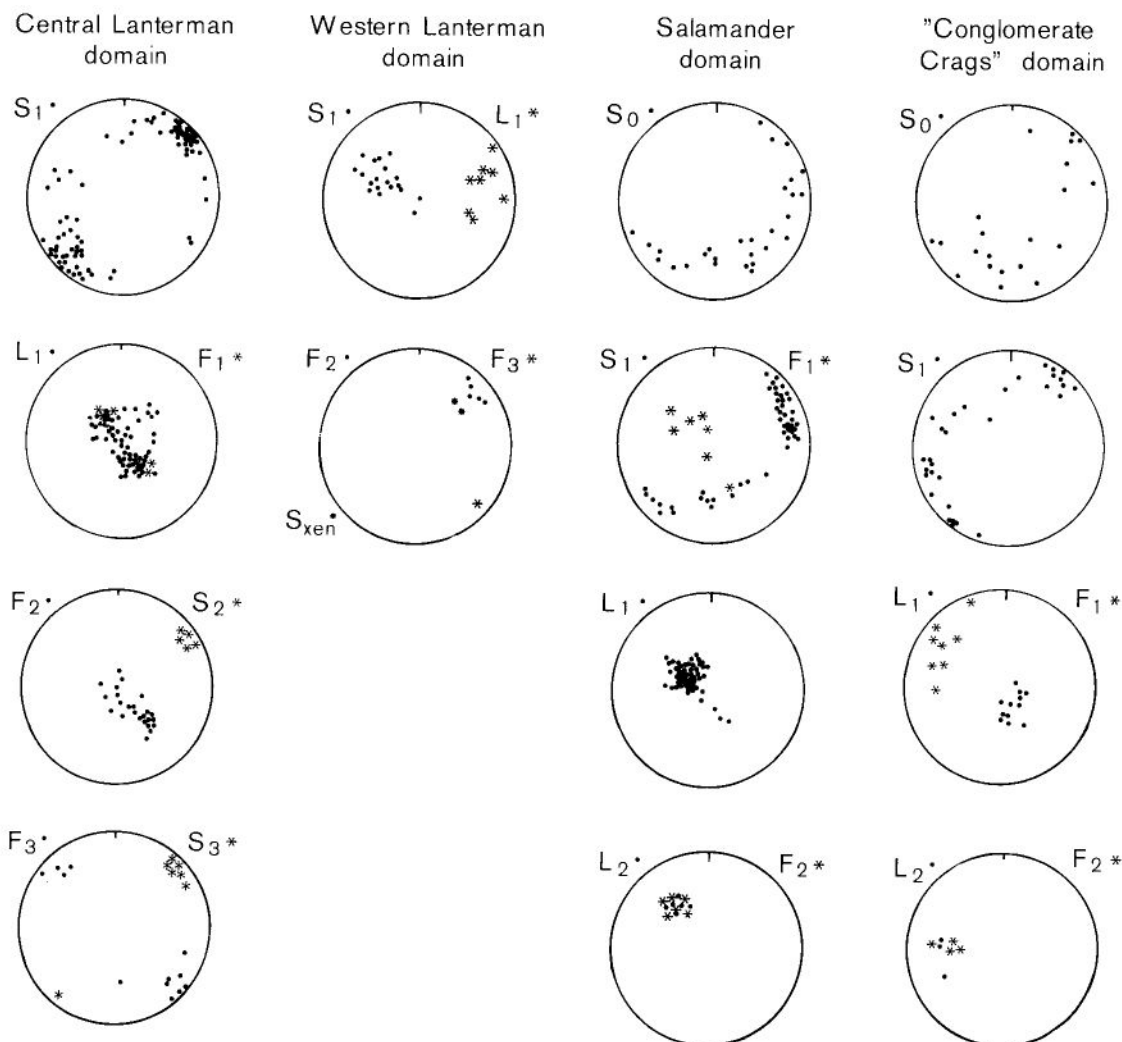


**Fig. 7** Geometric data from each of the four structural domains in the Lanterman Metamorphic Complex. All S-surfaces are plotted as poles.

the S<sub>1</sub> fabric and is interpreted to result from early D<sub>1</sub> development, because the early fabric is not observed as an axial fabric to folds in the compositional layering, and because it is never observed to be folded about F<sub>1</sub> folds in the compositional layering. Furthermore, the fact that quartz veins are not as tightly folded as F<sub>1</sub> folds in compositional layers in the same outcrop, suggests that quartz veins developed at some stage after the initiation of D<sub>1</sub>.

Two, prominent, variably developed crenulation sets deform S<sub>1</sub>. The earlier crenulation set (F<sub>2</sub>) plunges steeply, subparallel to L<sub>1</sub>, with its axial

crenulation cleavage (S<sub>2</sub>) subparallel to S<sub>1</sub>. The second crenulation set (F<sub>3</sub>) has subhorizontal axes and an axial cleavage (S<sub>3</sub>) subparallel to both S<sub>1</sub> and S<sub>2</sub> (Fig. 8C). Muscovite, which commonly overgrows fibrolite in unit 3 schists, is typically developed in S<sub>3</sub>. Map-scale reorientation of S<sub>1</sub> from its dominant northwest trend at Mount Bernstein and "Fibrolite Ridge" (Fig. 2) results in the observed scatter in S<sub>1</sub> (Fig. 7). This reorientation is due to flexures about subvertical axes which parallel the F<sub>2</sub> crenulations. No macroscopic F<sub>3</sub> folds have been observed in the central Lanterman domain.

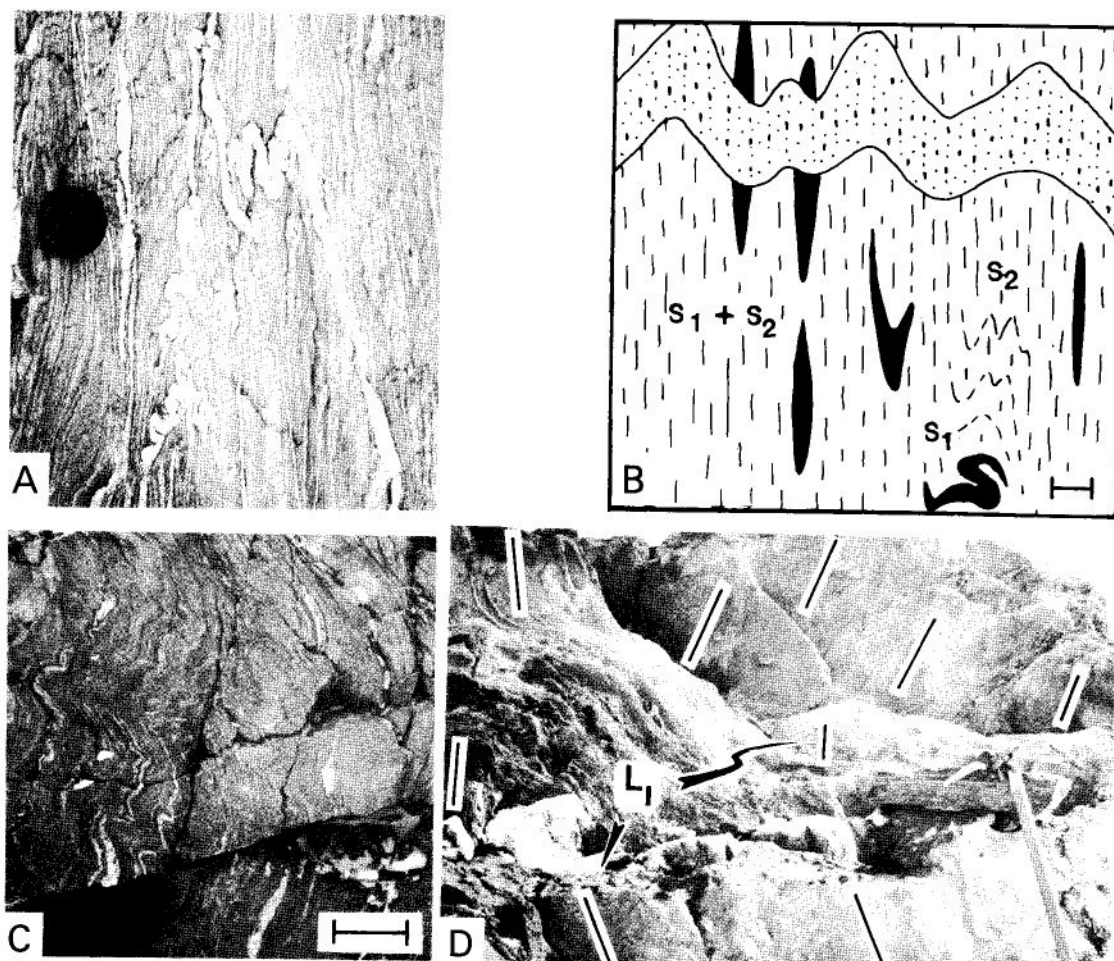


**Fig. 8** **A**  $F_1$  folds in quartz veins, with an axial  $S_1$  schistosity parallel to transposed compositional layering, Salamander Range. **B** Sketch of  $F_1$  folds and  $F_2$  crenulations in quartz veins (dark) and granite veins (dotted). The distinction between  $S_1$  and  $S_2$  is only apparent where  $F_2$  crenulations are developed. These relationships suggest that  $S_2$  crenulation accompanied the latest stages of  $S_1$  development in adjacent layers, as  $F_1$  and  $F_2$  folds in the granite veins are indistinguishable. Bar scale is 5 cm. **C**  $F_3$  crenulations in biotite schist, "Rutile Ridge". Bar scale is 10 cm. **D**  $L_1$  lineation (arrowed) on adjacent parallel  $S_1$  surfaces shows variable orientation which is interpreted to result from strain inhomogeneity on the scale of individual foliae, Salamander Range.

The differentiation of  $S_1$  and  $S_2$  fabrics is somewhat arbitrary where  $S_1$  has been selectively overprinted by the subparallel  $S_2$  (Fig. 8B). The  $S_2$  crenulations are most abundant adjacent to quartz veins and granite dikes which, as passive fabric elements, must have imparted a competency contrast to the rock body. The relationships illustrated in Fig. 8B are interpreted to indicate that  $S_1$  and  $S_2$  formed during continuous deformation in an essentially constant regime, with crenulations only being propagated where the early-formed foliation intersected rocks differing in competency.

The hornblende schists which occur as pods within unit 4 metasediments are typically strongly deformed. Fine-grained mylonitic fabrics at the margins of these pods provide evidence of intense strain localisation (Fig. 9A, B). The mylonitic fabric is parallel to  $S_1$ , and is defined by mineral assemblages identical to those within the less intensely deformed interiors of the pods. The mylonitic fabric is, however, locally folded into isoclines (Fig. 6B), and provides further evidence for localised complexities in the development of the  $S_1$  fabric.

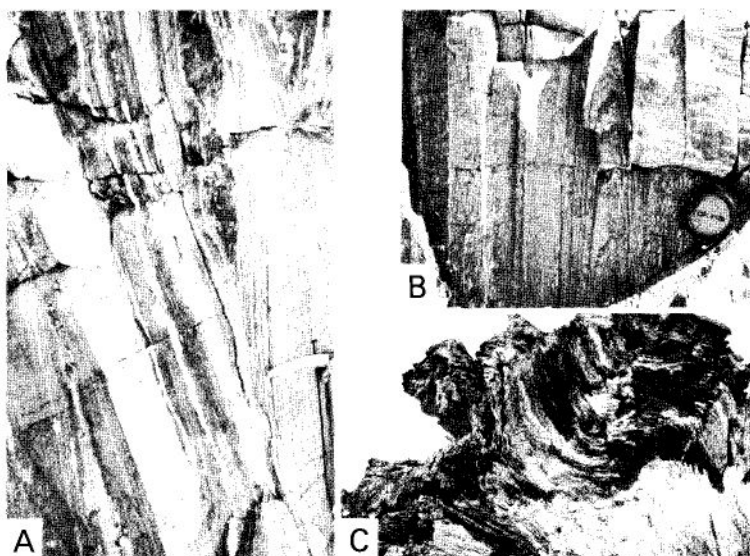


**Fig. 9** **A** Intense deformation manifest as boudinage and discordant foliations at the margin of amphibolite pod, "Fibrolite Ridge". **B** Folded mylonitic fabric in amphibolite, "Fibrolite Ridge". **C**  $F_3$  folds within chlorite schist, "Fibrolite Ridge" (outcrop is viewed from the north).

Subhorizontal  $F_3$  crenulations and associated mesoscopic folds are locally abundant in the chlorite and serpentine-talc schists (Fig. 9C). The vergence (Z-shaped viewed from the north) of  $F_3$  crenulations is consistent throughout.

#### The western Lanterman domain

The metasediments cropping out adjacent to the Lanterman Granodiorite in the western Lanterman Range are anomalous in that they dip at moderate angles to the southeast (Fig. 2 and 7) but are otherwise similar (structurally) to those in the central Lanterman domain. The transition to the steep-dipping central Lanterman domain is abrupt, occurring within a 30 m wide snow-covered pass. Both  $L_1$  and  $F_2$  structures are reoriented with respect to the central Lanterman domain (Fig. 7), thus, reorientation may have occurred about shallow northeast-plunging  $F_3$  structures. However, there are few  $F_3$  crenulations in this region, and the anomalous orientation may be due to another, otherwise unrecognised, generation of folds, or to faulting.

The metatonalite locally contains a strong foliation (Fig. 6B). Quartz-plagioclase veinlets oblique to the foliation are a distinctive feature of strongly foliated zones (Fig. 6B). The gneissic foliation is parallel to, and interpreted to be equivalent with,  $S_1$  in the adjacent metasediments.

The granites and granodiorites in the vicinity of "Termination Peak" show foliations defined by the elongation of xenoliths and, less commonly, tec-

tonic foliations (Fig. 6F). Both foliations dip to the southwest at 40–50° and are thus subparallel to the dominant trend of  $S_1$  in the Lanterman Metamorphic Complex (Fig. 7).

#### The Salamander domain

The Salamander Metamorphics form a steeply west-dipping sequence resembling the central Lanterman domain. The pervasive  $S_1$  schistosity parallels the transposed compositional layering. Deviation from westerly dips was found only along the western spur of Mount Pedersen where a macroscopic northwest-plunging second-generation fold results in the observed girdle in  $S_0$  and  $S_1$  (Fig. 7).  $L_1$ , which is identical to the extension lineation in the central Lanterman domain, typically plunges down dip in  $S_1$ . Its orientation is constant within any one foliation plane, but significant variation (up to 25°) is common between adjacent planes (Fig. 8D). Re-orientation of  $S_0$  and  $S_1$  is not observed. Such relationships could imply refolding about an axis perpendicular to the schistosity, but as such folds have not been observed elsewhere in the Lanterman Metamorphic Complex, the variation in  $L_1$  is thought to represent a distribution acquired during  $L_1$  formation and implies inhomogeneity in  $D_1$  strain on the scale of individual foliae.

#### The "Conglomerate Crags" domain

The metaconglomerates cropping out along the eastern margin of the Lanterman Range exhibit both facing and vergence. It is thus possible to resolve the macroscopic structure of this region,

**Table 1** Strain determinations based on clast shape in metaconglomerates, "Conglomerate Crags".

Conglomerate	Clast type	X:Z	Y:Z	X:Y:Z (average)
Felsic conglomerate	felsic	106:9; 193:17; 85:8	85:10; 153:17	11:9:1
Mafic conglomerate	amphibolite	230:78; 130:13; 75:19; 65:9	123:33; 75:28; 93:37; 64:24	6:3:1
	quartz	220:27; 115:32	78:26; 75:55; 80:27; 85:30	8:2.5:1
	granite	100:21	45:31; 31:52; 26:21	5:1:1

which includes a syncline exposed in the cliffs beneath "Conglomerate Crags". There is a marked contrast between the style of  $S_1$  and the nature of folding in the felsic and mafic metaconglomerates (units 5 and 6).

Within the felsic metaconglomerate (unit 5),  $S_1$  is the dominant foliation. It is defined by the preferred orientation of oblate spheroid shaped felsic clasts (Fig. 4A). Both X and Y exceed Z by a factor of nine or more (where X, Y and Z represent the maximum, intermediate, and minimum finite strain axes respectively) with the spheroids elongated ( $L_1$  parallel to X) in the dip direction of  $S_1$  (Table 1). Unlike the central Lanterman domain, the primary sedimentary layering, defined by psammitic intercalations, is not transposed. Mesoscopic folds to which  $S_1$  is axial have not been observed.  $S_1$  parallels the compositional layering throughout most of the outcrop section. However, discordance between  $S_0$  and  $S_1$  occurs within 5 m of the eastern margin of the felsic conglomerate (Fig. 4A). The  $S_1/S_0$  intersection plunges gently north, perpendicular to the long axes of the clasts, while vergence is synformal to the east. In the matrix of the conglomerate,  $S_1$  is defined by elongation of actinolite, chlorite, and/or biotite.

Second generation asymmetric folds with subvertical axes (identical to the fold figured by Bradshaw et al. 1982, fig. 3) occur locally within the felsic conglomerates (Fig. 4B). Third generation crenulations intersecting the  $S_2$  at high angles occur locally in the metaconglomerate (Fig. 4C) and more commonly in the intercalated metapsammites.

The mafic metaconglomerates exhibit a pronounced L-tectonite fabric ( $L_1$ ) defined by the elongation of prolate spheroid shaped mafic clasts (Fig. 4A, B).  $L_1$  pitches steeply southeast within  $S_1$  and is perpendicular to the intersection of  $S_1$  and  $S_0$ . This intersection is readily observed in the numerous psammitic intercalations. All clast types are prolate spheroids (Table 1), with some evidence for compositional dependence of strain (felsic clasts are typically more strained than mafic clasts in the same outcrop). The gross differences in clast shape between the mafic and felsic metaconglomerates is

probably a function strain inhomogeneity, related to the development of the macroscopic  $F_1$  structure (Fig. 1), with the limb region (felsic metaconglomerate) of this  $F_1$  structure more intensely flattened than the hinge region (mafic metaconglomerate).

A reversal in the vergence of the shallow north-plunging folds, and in the  $S_1/S_0$  intersection, indicates the presence of a large  $F_1$  syncline at "Conglomerate Crags" (Fig. 5C). Cross beds have been observed on both limbs of this closure and confirm that it is synclinal. Vergence remains unchanged throughout the predominantly overturned eastern limb, up to, and including, the last outcrop prior to the Bowers Group sediments on Reilly Ridge (Laird et al. 1982).

Laird et al. (1982) recorded a 370 m thick section of eastward-younging Husky Conglomerate between "Conglomerate Crags" and Reilly Ridge. Although I have not been able to determine younging in the easternmost 400 m (only two reliable cross beds have been identified on the eastern limb of the  $F_1$  syncline), the consistent vergence within this limb (synclinal to the west) indicates that all rocks at this locality young westwards.

Reorientation of  $S_0$  and  $S_1$  about a shallow south-east-plunging (? $F_3$ ) flexure in the vicinity of the proposed Husky unconformity (Wodzicki et al. 1982) is responsible for the observed scatter in  $S_0$  and  $S_1$  in the "Conglomerate Crags" domain (Fig. 7).

## DISCUSSION

The sequence of stratigraphic, structural, metamorphic, and intrusive events observed in the Lanterman Metamorphic Complex is summarised in Table 2. The ages of many of these events are constrained by regional tectonic relationships (Tessensohn et al. 1981; Bradshaw et al. 1982) and by the isotopic data of several intrusive (Kreuzer et al. 1981) and metamorphic (Adams et al. 1982) rocks from the Lanterman Range.

In the central and western Lanterman Range, and in the Salamander Range, the earliest recognised deformation phase ( $D_1$ ), which ultimately resulted

**Table 2** Geologic history of the Lanterman Metamorphic Complex.

Western terrane	Eastern terrane	Age
Salamander, western Lanterman, and central Lanterman structural domain	"Conglomerate Crags" structural domain and talc schists	
i. Deposition of sequence consisting dominantly of semipelitic sediments with subordinate pelitic and calcareous sediments and, possibly, eruption of minor volcanics.	1. Deposition of conglomerates.	?
2. Intrusion of precursors of metatonalites and associated hornblende dikes.		?
3. Prograde amphibolite facies metamorphism, $D_1$ , intrusion of Lanterman Granodiorite.	2. Emplacement of ultramafic schists (of possible oceanic origin), greenschist facies metamorphism, $D_1$ .	480–500* (Ross event)
4. Retrogressive amphibolite–greenschist facies metamorphism, $D_2$ .	3. $D_2$ , greenschist facies metamorphism.	(Ross event)
5. Retrogressive greenschist facies metamorphism, $D_3$ .	4. $D_3$ , reactivation of talc schists, greenschist facies metamorphism.	350–450†

\*Kreuzer et al. (1981); †Adams et al. (1982).

in the development of the  $S_1$ ,  $F_1$  and  $L_1$  fabric elements, was a complex event accompanied by regional amphibolite-grade metamorphism. Where unaffected by subsequent deformation,  $S_1$  is subvertical and northwest trending. It is axial to folds in compositional layers, in quartz veins, and in granite dikes.  $F_1$  fold tightness increases from granite dikes through quartz veins to compositional layers, indicating that substantial  $D_1$  strain accumulated prior to the intrusion of the dikes. However, the occurrence of  $S_1$  as an axial schistosity in these dikes indicates that  $D_1$  outlasted the emplacement of these granitoids. Further evidence for complexities in the overall development of  $D_1$  fabrics includes the preservation of a relict mica fabric adjacent to  $F_1$  hinges in quartz veins and the variation in  $L_1$  in adjacent  $S_1$  foliae (Fig. 8D).

In summary, the  $S_1$  schistosity and the associated  $F_1$  folds in the central Lanterman Range are regarded as the product of a prolonged deformation resulting principally from east–west shortening. The deformation was initiated prior to the emplacement of the Lanterman Granodiorite. During the deformation, the compositional layering was transposed in most of the Lanterman Metamorphics, a pervasive steep-dipping schistosity and associated near-vertical mineral elongation lineation developed, and quartz was concentrated into veins. Continued deformation during granite intrusion resulted in folds of varying tightness in

the granite dikes and, finally, the local crenulation of the schistosity.

The typically crenulate form of  $F_3$  folds in the talc schists cropping out near the eastern margin of the Lanterman Metamorphic Complex is reminiscent of structures associated with late-stage faulting (Wilson et al. 1982). The west-up vergence of the structures within these zones suggests that they are related to movement on the faults which define the eastern boundary of the Lanterman Metamorphic Complex. The absence of cataclasis within the  $D_3$  zones and the greenschist facies (chlorite–talc–serpentine grade) assemblages preserved in  $S_3$  crenulations are indicative of relatively deep-level ductile activation of these faults. Significant displacements across these zones are implied by the juxtaposition of terranes of different metamorphic, structural, sedimentological, and intrusive histories. In particular, the reduction in the metamorphic grade, from amphibolite (sillimanite-K feldspar) in the western terrane, to greenschist in the eastern terrane, suggests that the talc-schist zone is associated with a crustal suture. This suggestion is consistent with the talc schists being of oceanic or mantle derivation tectonically inserted into the Lanterman Metamorphic Complex. Therefore, the outcrop of these talc schists may delimit a fundamental tectonic discontinuity, and consequently the metaconglomerates in the eastern terrane are probably not conformable with

the higher grade metamorphics in the core of the Lanterman Range.

The age of deformation in the talc-schist zones, and the age of their emplacement, remains poorly constrained. Adams et al. (1982) have recorded K-Ar mineral ages between 450 Ma and 350 Ma from amphibolites near Husky Pass which possibly correspond to the D<sub>3</sub> event. It is likely, however, that these zones have responded to repeated movements during the excavation of the Lanterman Metamorphics, and the Middle Devonian ages may reflect only reactivation events. In orogenic belts in which ultramafic schists separate distinct terranes (often representing different continents), the structural geometry on either side of the sutures are similar and are frequently dominated by steep foliations with subvertical stretching lineations (Burg & Chen 1984), a geometry which reflects strain associated with the closure of a suture. Thus, the emplacement of the talc schists may have been coeval with the formation of the steeply plunging linear fabrics elsewhere in the Lanterman Range. In the western terrane, these fabrics (L<sub>1</sub>/L<sub>2</sub>) are demonstrably associated with the emplacement of the Ross-aged Lanterman Granodiorite (Fig. 8).

The principal deformation episode which was responsible for both D<sub>1</sub> and D<sub>2</sub> structures recognised in the Lanterman Metamorphic Complex is believed to have been essentially coeval with the intrusion of the Lanterman Granodiorite. The 480–490 Ma Rb/Sr age of these intrusives (Kreuzer et al. 1981) constrains the age of this deformation to the latest Cambrian and/or earliest Ordovician.

In light of evidence for extensive Late Cambrian and possibly Early Ordovician sedimentation in the adjacent Bowers Group, Cambro-Ordovician tectonism in the Lanterman Range is difficult to reconcile with the existence of an unconformity between the Lanterman Metamorphics and the Husky Conglomerate (Laird & Bradshaw 1983). While this study has failed to provide evidence for this unconformity near the proposed type locality (Laird et al. 1982), its existence has apparently been confirmed by recent investigations in other parts of the Lanterman Range (Weaver et al. 1984). In view of the evidence that: (1) the amphibolite-grade metamorphics exposed to the west of the talc schists in the Lanterman Range (i.e. the western terrane) were uplifted some 10–25 km during the Late Cambrian and/or Early Ordovician (Grew & Sandiford 1984), and (2) the Bower Supergroup forms part of an intraoceanic arc (Weaver et al. 1984), the apparent preservation of an unconformity between the Husky Conglomerate and metaconglomerates supports the argument that the Lanterman Metamorphics represent a composite of two tectonically distinct terranes. This interpretation

suggests that the talc schists represent a previously unrecognised tectonic discontinuity which separates two terranes, a western and an eastern terrane, of fundamentally distinct character. This discontinuity is believed to be as significant as, if not more than, the unconformity beneath the Husky Conglomerate, and it raises the possibility that the deformed metaconglomerates in the western Lanterman Range may form part of the Bowers arc.

#### ACKNOWLEDGMENTS

I am indebted to Dr E. S. Grew for the opportunity to join the northern Victoria Land field trip as part of a project supported by U.S. National Science Foundation Grant DPP 80-19527 to the University of California, Los Angeles, and for numerous "in field" discussions. The logistic support provided by the 1981–82 USARP and, particularly, Dr E. Stump, which enabled the smooth running of all field operations, is gratefully acknowledged. Drs E. S. Grew, J. D. Bradshaw and C. J. Wilson are thanked for their comments on an earlier draft of this manuscript.

#### REFERENCES

- Adams, C. J.; Gabites, J. E.; Wodzicki, A.; Laird, M. G.; Bradshaw, J. D. 1982: Potassium-argon geochronology of the Precambrian–Cambrian Wilson and Robertson Bay Groups and Bowers Supergroup, North Victoria Land, Antarctica. In: Craddock, C. ed. Antarctic geoscience. Madison, University of Wisconsin Press. Pp. 543–548.
- Bradshaw, J. D.; Laird, M. G. 1983: The Pre-Beacon geology of northern Victoria Land: a review. In: Oliver, R. L.; James, P. R.; Jago, J. B. ed. Antarctic earth science. Canberra, Australian Academy of Science. Pp. 98–101.
- Bradshaw, J. D.; Laird, M. G.; Wodzicki, A. 1982: Structural style and tectonic history in northern Victoria Land. In: Craddock, C. ed. Antarctic geoscience. Madison, University of Wisconsin Press. Pp. 809–816.
- Burg, J. P.; Chen, G. M. 1984: Tectonics and structural zonation of southern Tibet. *Nature* 311: 219–223.
- Dow, J. A. S.; Neall, V. E. 1974: Geology of the lower Rennick Glacier, northern Victoria Land, Antarctica. *New Zealand journal of geology and geophysics* 17: 659–714.
- Grew, E. S.; Sandiford, M. 1982: Field studies of the Wilson and Rennick Groups, Rennick Glacier area, northern Victoria Land. *Antarctic journal of the United States* 17: 7–8.
- 1984: A staurolite-talc assemblage in tourmaline - phlogopite - chlorite schist from northern Victoria Land, Antarctica, and its petrogenetic significance. *Contributions to mineralogy and petrology* 87: 337–350.

- 1985: Staurolite in a garnet - hornblende - biotite schist from the Lanterman Range, northern Victoria Land, Antarctica. *Neues Jahrbuch für Mineralogie, Monatshefte*, Heft 9.
- Kleinschmidt, G. 1981: Regional metamorphism in the Robertson Bay Group area and in the southern Daniels Range, North Victoria Land, Antarctica—a preliminary comparison. *Geologisches Jahrbuch Reihe B Heft 41* : 201–228.
- Kleinschmidt, G.; Skinner, D. N. B. 1981: Deformation styles in the basement rocks of North Victoria Land, Antarctica. *Geologisches Jahrbuch Reihe B Heft 41* : 155–199.
- Kreuzer, H.; Hohndorf, A.; Lenz, H.; Vetter, U.; Tessensohn, F.; Müller, P.; Jordan, H.; Harre, W.; Besang, C. 1981: K/Ar and Rb/Sr dating of igneous rocks from North Victoria Land, Antarctica. *Geologisches Jahrbuch Reihe B Heft 41* : 267–273.
- Laird, M. G.; Bradshaw, J. D. 1983: New data on the Lower Palaeozoic Bowers Supergroup, northern Victoria Land. In: Oliver, R. L.; James, P. R.; Jago, J. B. ed. Antarctic earth science. Canberra, Australian Academy of Science. Pp. 123–126.
- Laird, M. G.; Bradshaw, J. D.; Wodzicki, A. 1982: Stratigraphy of the Upper Precambrian and Lower Palaeozoic Supergroup, northern Victoria Land, Antarctica. In: Craddock, C. ed. Antarctic geoscience. Madison, University of Wisconsin Press. Pp. 535–542.
- Sturm, A.; Carryer, S. J. 1970: Geology of the region between Matusevich and Tucker Glaciers, North Victoria Land. *New Zealand journal of geology and geophysics* 13 : 408–435.
- Tessensohn, F.; Duphorn, K.; Jordan, H.; Kleinschmidt, G.; Skinner, D. N. B.; Vetter, U.; Wright, T. O.; Wyborn, D. 1981: Geological comparison of the basement units in North Victoria Land, Antarctica. *Geologisches Jahrbuch Reihe B Heft 41* : 31–88.
- Weaver, S. D.; Bradshaw, J. D.; Laird, M. G. 1984: Geochemistry of the Cambrian Volcanics of the Bowers Supergroup and implications for the early Palaeozoic tectonic evolution of northern Victoria Land, Antarctica. *Earth and planetary science letters* 54 : 346–356.
- Wilson, C. J. L.; Harris, L. B.; Richards, A. L. 1982: Structure of the Mallacoota area, Victoria. *Journal of the Geological Society of Australia* 29 : 91–105.
- Wodzicki, A.; Bradshaw, J. D.; Laird, M. G. 1982: Petrology of the Wilson and Robertson Bay Groups and Bowers Supergroup, northern Victoria Land, Antarctica. In: Craddock, C. ed. Antarctic geoscience. Madison, University of Wisconsin Press. Pp. 549–554.
- Wyborn, D. 1981: Granitoids of North Victoria Land—field and petrographic observations. *Geologisches Jahrbuch Reihe B Heft 41* : 229–249.